NACA TN No. 1623

NATIONAL ADVISORY COMMITTEE FOR AERONAUTICS

TECHNICAL NOTE

NO. 1623

SOME FUNDAMENTAL SIMILARITIES BETWEEN BOUNDARY-LAYER FLOW AT TRANSONIC AND LOW SPEEDS

By Gerald E. Nitzberg and Stewart Crandall

Ames Aeronautical Laboratory
Moffett Field, Calif.

WASHINGTON
JUNE 1948

NATIONAL ADVISORY COMMITTEE FOR AERONAUTICS

TECHNICAL NOTE NO. 1623

SOME FUNDAMENTAL SIMILARITIES BETWEEN BOUNDARY-LAYER FLOW AT TRANSONIC AND LOW SPEEDS

By Gerald E. Nitzberg and Stewart Crandall

SUMMARY

An analysis of low-speed boundary-layer flow over airfoils at moderate angles of attack and at Reynolds numbers of several million is presented. Methods are developed for estimating the growth of the boundary layer in the regions of laminar separation and transition. Calculation of the growth of the turbulent boundary layer and the chordwise location of the turbulent separation point are considered.

The concepts, which are found to be basic for understanding low-speed boundary-layer flow, are also applied to data for transonic speeds. A close similarity is found to exist between low-speed and transonic boundary-layer flow. An approximate procedure for calculating boundary-layer growth through shock waves is presented. The local effects of both laminar and turbulent boundary-layer separation are considered.

INTRODUCTION

Experimental measurements at transonic speeds have indicated that changes in the airfoil surface condition or of Reynolds number cause marked changes in the chordwise static-pressure distribution. In particular, the flow in the vicinity of the shock wave is entirely different for laminar than for turbulent boundary-layer flow. Before an adequate analysis of transonic flow past airfoil sections can be made, it is necessary to obtain some understanding of the characteristics of boundary layers at transonic speeds.

There is little analysis available for boundary layers at transonic speeds; however, a vast literature dealing with low-speed boundary-layer theory exists. The question naturally arises as to whether some of these numerous methods of analysis can be extended

to apply to transonic flow. The various boundary-layer flow regimes at low speeds are considered for the case of an airfoil at a moderate angle of attack. A number of basic characteristics of boundary-layer flow appear in this analysis. It is the purpose of this report to examine some transonic boundary-layer data to determine whether fundamental similarity exists between boundary-layer flow at low and transonic speeds.

An airfoil at a moderate angle of attack was selected for the low-speed case in order to avoid the complex problem of predicting the chordwise location of transition from laminar to turbulent flow when this occurs ahead of the theoretical position of laminar separation. In the case considered, transition from laminar to turbulent flow follows separation of the laminar boundary layer and subsequent reattachment of the flow to the airfoil surface. This case is fruitful because regions of both laminar and turbulent separation occur.

There are several semiempirical methods for calculating the development of the turbulent boundary layer and the position of turbulent separation. Data obtained at the Bureau of Standards and recently presented by Dryden (reference 1) assist in evaluating the methods for calculating turbulent separation. These data show that the skin-friction coefficient of turbulent boundary layers is highly dependent upon the velocity profile, that is, the shape of the velocity distribution through the boundary layer. This dependence was not established at the time von Doenhoff and Tetervin (reference 2) developed their semiempirical equation for calculating the chordwise position of turbulent separation. It appears that the complexity of their equation is at least partly due to attempting to fit an equation to the experimental data while neglecting the dependence of skin-friction coefficient on the velocity profile. The much simpler procedure developed by Gruschwitz (reference 3) is in substantial agreement with the data of reference 1 and is a fair approximation to the data of reference 2. Therefore, the semiempirical equation of Gruschwitz is used in the present report for calculating the turbulent separation point.

A significant experimental study of boundary-layer flow at transonic speeds has been made by Ackeret, Feldmann, and Rott (reference 4.) These data are considered in the present report in terms of the concepts developed for low-speed flows.

SYMBOLS

c	airfoil chord length
h	surface bump height

H ratio of boundary-layer displacement to momentum thickness (δ^*/θ)

L length of region of laminar separation

M ratio of local velocity to local velocity of sound

M^* ratio of local velocity to critical velocity of sound

p static pressure

p_o total head

q dynamic pressure

R_c Reynolds number based on airfoil chord $\left(\frac{U_o c}{\nu}\right)$

R_θ Reynolds number based on boundary-layer momentum thickness $\left(\frac{U\theta}{\nu}\right)$

S pressure coefficient $\left(\frac{U}{U_o}\right)^2$

u local velocity in boundary layer

U local velocity outside boundary layer

U_o free-stream velocity

ΔU maximum perturbation velocity

x chordwise distance

y distance normal to surface

β velocity gradient $\left[\frac{d\sqrt{S}}{d(x/c)}\right]$

δ total boundary-layer thickness

δ^* boundary-layer displacement thickness

$$\left[\delta^* = \int_o^\delta \left(1 - \frac{\rho_u}{\rho}\frac{u}{U}\right) dy\right]$$

ρ density outside boundary layer

ρ_u density in boundary layer at point where velocity equals u

θ boundary-layer momentum thickness

$$\left[\theta = \int_0^{\delta} \frac{\rho_u u}{\rho U} \left(1 - \frac{u}{U} \right) dy \right]$$

η Gruschwitz boundary-layer shape parameter (equation (6))

τ_o surface shearing stress

$\tau_o/2q$ skin-friction coefficient

ν kinematic viscosity

ANALYSIS OF LOW-SPEED BOUNDARY-LAYER FLOW

Consider a smooth-surfaced airfoil at a moderate angle of attack in a low-turbulence low-speed flow. The various regimes of boundary-layer flow over the airfoil can be readily differentiated on the basis of the local pressure distribution. To avoid the confusion of plus and minus signs, the pressure coefficient S, which is defined as the ratio of the local to the free-stream velocity squared, will be used. The maximum pressure coefficient occurs on the upper surface near the airfoil leading edge. (See fig. 1.) Over the next few percent of the airfoil chord, there is an abrupt decrease in S. This decrease occurs in two parts which are divided by a short region of constant pressure. The corresponding behavior of the boundary layer is as follows: From the peak pressure point to the constant-pressure region the flow is laminar. In the region of constant pressure, which will be shown to be about 1 percent of the chord in length for Reynolds numbers of about one million, the boundary layer remains laminar but is separated from the surface by a "dead-air" bubble. The flow then turns turbulent and spreads back to the surface with the accompanying second abrupt decrease in S. Aft of the sharp forward pressure peak there are relatively moderate chordwise pressure gradients (fig. 1) and the boundary layer is turbulent. Over the rear portion of the airfoil there is a region of relatively constant pressure. In such a region, S is somewhat greater than one, and the local boundary-layer flow is referred to as turbulent separation.

The pressure distribution which has just been described is the actual viscous-flow pressure distribution which approximates the potential-theory pressure distribution except in the vicinity of both the region of laminar and turbulent separation.

The various regimes of flow will now be treated in detail.

Laminar Flow

The extent of the laminar flow on the airfoil for the case being considered is small but it is of importance for determining the initial conditions in the turbulent boundary layer. In reference 5, von Kármán and Millikan have studied laminar boundary-layer separation for the case of pressure distributions having a sharp peak. It is shown in this reference that the conditions for laminar separation are independent of both Reynolds number and the actual magnitude of the peak pressure coefficient. When the maximum pressure occurs near the leading edge, as in the present case, the laminar boundary layer separates at the chordwise station at which the local value of S is about 0.81 times the peak pressure coefficient. Furthermore, as can be determined from the results of reference 5, the local boundary-layer momentum thickness at this separation point is simply

$$\frac{\theta}{c} = \frac{0.4}{\sqrt{R_c \beta}} \tag{1}$$

where c is the chord length, R_c is the airfoil Reynolds number, and β is defined as

$$\beta = \frac{d\sqrt{S}}{d(x/c)} \equiv \frac{d(U/U_o)}{d(x/c)}$$

For the low-speed type of airfoil pressure distribution being analyzed in the present report, the value of β is nearly constant from the pressure peak to the laminar separation point so that equation (1) is applicable. From reference 5, it is also found that at the laminar separation point the ratio of boundary-layer displacement to momentum thickness has a value of 3.8.

A region of separated laminar flow is characterized by constant local pressure. Thus, as there are no pressure or shear forces acting on the boundary layer, there cannot be any appreciable changes in the boundary-layer momentum defect; that is, the boundary-layer momentum thickness must remain virtually constant over the constant-pressure region. At the same time there must be a rapid local increase in the boundary-layer displacement thickness since it is necessary to have a distortion of the streamlines to decrease the local pressure gradient to zero. In reference 6, laminar separation was measured on an NACA 66,2-216 airfoil section at an angle of attack of 10.1° and for a Reynolds number range of 0.9 to 2.6 million. An analysis of these data indicated that the momentum thickness does remain virtually constant

in the region of constant pressure while there is a marked increase in the boundary-layer displacement thickness. (See fig. 2.)

There appears to be the following factor determining the magnitude of this increase in the displacement thickness. Throughout the range of Reynolds numbers for which data are presented, the length of the region of constant pressure can be characterized by a value of R_L equal to approximately 25,000, where R_L is the length of the region of constant pressure times the local velocity and divided by the kinematic viscosity. Two other properties of the laminar separated region are known: The local pressure, hence velocity, are constant; whereas in the absence of separation there would be a large local velocity gradient β. The shape and magnitude of the dead-air bubble are such as to bring about this change in the local velocity gradient. From thin airfoil theory, it is known that a local velocity perturbation is proportional to the height of a local bump

$$\frac{h}{L} = K \frac{\Delta U}{U} \tag{2}$$

where

h height of bump

ΔU velocity perturbation due to bump

U local stream velocity

L length of region of constant velocity characterized by $R_L = 25{,}000$

The following data obtained from reference 6 indicate that the value of K is about one:

Reynolds number	$\frac{\Delta U}{U}$	$\frac{h}{L}$
0.9×10^6	0.10	0.08
1.5×10^6	.10	.08
2.2×10^6	.08	.07

The height of the dead-air bubble is thus directly determinable from the potential-theory pressure distribution and equation (2). That this height is equal to the increment of the displacement thickness over the constant-pressure region follows directly from the definition of the displacement thickness, since the air velocity inside the bubble is virtually zero.

The boundary-layer momentum and displacement thickness at the end of the region of laminar separation are thus calculable. The local momentum thickness is obtained from equation (1), and the displacement thickness is 3.8 times this value plus the maximum displacement of the separated flow from the surface. The latter quantity is obtained from equation (2).

Transition Region

At the termination of the short constant-pressure region, the separated laminar flow becomes turbulent and spreads back toward the airfoil surface. Over the region in which the separated turbulent flow spreads toward the airfoil surface to establish itself as a turbulent boundary layer, there is a large pressure gradient. An analysis of the experimental boundary-layer profiles in reference 6 indicated that over this region there was only a small variation in the boundary-layer displacement thickness. This variation consisted of an initial decrease followed by an increase, so that the displacement thickness at the end of this region of large pressure gradient was nearly the same as at the beginning. At the same time, the boundary-layer momentum thickness increased rapidly. The classical equation for analyzing the growth of momentum thickness is the boundary-layer momentum integral equation

$$\frac{d\theta}{dx} + \frac{(2\theta+\delta^*)}{2S}\frac{dS}{dx} = \frac{\tau_o}{2q} \qquad (3)$$

where

θ momentum thickness

x length along airfoil surface

δ^* displacement thickness

S pressure coefficient

q local dynamic pressure

$\tau_o/2q$ skin-friction coefficient

The growth of the boundary-layer momentum thickness in the transition region can be calculated by means of equation (3). This calculation is simple because when the flow is detached from the surface the skin-friction coefficient is zero; moreover the experimental data suggest the use of a constant value of the boundary-layer

displacement thickness, namely, its value at the end of the region of laminar separation. Hence equation (3) reduces to

$$\left(\frac{2\theta_1+\delta_1^*}{2\theta_2+\delta_1^*}\right) = \frac{S_2}{S_1} \qquad (4)$$

where subscripts 1 and 2 indicate, respectively, conditions at the beginning of and at some later point in the transition region.

In figure 2, a comparison is presented between the theoretical and experimental momentum thickness distribution in the region of laminar separation and transition for the NACA 66,2-216, a = 0.6 airfoil section at an angle of attack of 10.1° and a Reynolds number of 900,000. According to the theory, the momentum thickness should remain constant over the region of separation at a value given by equation (1). In the transition region the momentum thickness growth was calculated by means of equation (4), using the experimental pressure distribution obtained from reference 6 and assuming a constant value of displacement thickness of 0.0009 chord lengths.

The value of momentum thickness at the point of laminar separation estimated, using equation (1), agrees well with the experimental value. However, there is a growth of momentum thickness in the region of constant pressure not predicted by the theory. Consequently, the theoretical values of momentum thickness in the following transition region are lower than the experimental because they depend upon the theoretical value at the end of the constant-pressure region which is somewhat lower than the experimental.

Turbulent Flow

A number of methods are available for calculating the growth of the turbulent boundary layer. These methods consist of different procedures for solving the boundary-layer momentum equation. The factors which appear in this equation are the chordwise pressure distribution, the local ratio of displacement to momentum thickness, and the local skin-friction coefficient. At points some distance ahead of the turbulent separation there is uncertainty in the theoretical estimation of each of these factors. The presence of a region of separated flow appreciably alters the pressure distribution, ahead of as well as behind the separation point, from the unseparated or potential-flow distribution. The ratio of displacement to momentum thickness varies from about 1.4 to 2.5 over the region of turbulent flow. The data recently presented by Dryden show that the variation of this ratio results in a marked variation in the skin-friction coefficient.

In spite of the previously mentioned difficulties, relatively simple approximate solutions of the momentum equation can be used to obtain quite accurate values for the boundary-layer growth up to the vicinity of the turbulent separation point. In cases where turbulent separation occurs, errors in evaluating the skin-friction coefficient are of secondary importance because the effects of the local pressure forces on the boundary-layer growth are larger than the surface shear forces. The ratio of displacement to momentum thickness δ^*/θ appears in the momentum equation only in the group $(\delta^*/\theta + 2)$ which, although ranging from 3.4 to 4.5, only varies between 3.4 and 3.8 for the major portion of the region of unseparated turbulent flow. It thus appears that the greatest uncertainty in the theoretical calculation of boundary-layer growth arises from changes in the pressure distribution due to the presence of a region of turbulent separated flow. The magnitude of these pressure changes depends upon the variation of the boundary-layer displacement thickness in the wake as well as over the rear portion of the airfoil. This is a complex problem which has not as yet been adequately solved. Of course, if the boundary-layer calculations are based on an experimental pressure distribution, this complexity is circumvented.

In view of the uncertainty in evaluating the basic parameters, it follows that elaborate step-by-step calculations of the boundary-layer growth involve unwarranted complexity. For fully developed, turbulent, boundary-layer flow, a reasonable value for the skin-friction coefficient can be obtained from Falkner's equation for turbulent flow over flat plates (reference 7), namely

$$\frac{\tau_o}{2q} = \frac{1}{153\ R_\theta^{1/6}}$$

where R_θ is the local Reynolds number in which the momentum thickness is used as the characteristic length. The chordwise variation of boundary-layer momentum thickness can be obtained most directly by substituting this equation into equation (3) and integrating under the assumption of a constant average value of H of 1.6 which leads to

$$\left(\frac{\theta}{c}\right)_2^{7/6} = \frac{0.0076}{R_c^{1/6} S_2^{2.1}} \int_{(x/c)_1}^{(x/c)_2} S^2 d\,(x/c) + \left(\frac{\theta}{c}\right)_1^{7/6} \left(\frac{S^1}{S_2}\right)^{2.1} \qquad (5)$$

A knowledge of the chordwise growth of boundary-layer momentum thickness gives no indication of separation. Boundary-layer measurements in the vicinity of the turbulent separation point are in general agreement that the boundary-layer shape parameter

($H = \delta^*/\theta$) can be used as an indicator of the location of the turbulent separation point. The value of H at separation is between 1.8 and 2.7, usually being about 2.5. Therefore, a relationship is needed to permit the calculation of the boundary-layer shape parameter. In reference 2, the semiempirical equation derived for calculating the variation of H is

$$\theta \frac{dH}{dx} = e^{4.680(H-2.975)} \left[-\frac{\theta}{S} \frac{dS}{dx} \frac{\overline{2q}}{\tau_o} - 2.035 \ (H - 1.286) \right]$$

where $\frac{\overline{\tau_o}}{2q}$ is the equivalent flat-plate skin-friction coefficient based on the local value of R_θ. It appears that this equation is excessively complex as a result of the fact that, in fitting an equation to the experimental data, it was assumed that the value of the skin-friction coefficient was independent of H. The data presented in reference 1 indicate that, for values of H from about 1.5 to 2.2, the skin-friction coefficient is approximately proportional to $(\overline{\tau_o/2q})/(H-1.29)$. Thus, when the dependence of skin-friction coefficient on H is taken into account the von Doenhoff-Tetervin equation may reduce to the much simpler form

$$F(H)dH = -\frac{dS}{S} \frac{2q}{\tau_o} - A \frac{dx}{\theta}$$

However, there are not sufficient data available to permit an accurate determination of the variation of skin-friction coefficient with H as well as with Reynolds number. In the present report the Gruschwitz equation will be used.

Gruschwitz assumed that the turbulent boundary-layer velocity profiles formed a one-parameter family. The shape parameter he used was defined as

$$\eta = 1 - \left(\frac{u}{U} \right)^2_{y=\theta} \tag{6}$$

This parameter is related to θ, x, and S by the empirical equation

$$\frac{\theta}{S} \frac{d(S\eta)}{dx} = 0.00461 - 0.00894 \ \eta$$

The data of references 1 and 2 lend considerable weight to the basic assumption of Gruschwitz. In both of these references, the velocity distribution through the boundary layer is shown to depend only upon H. The variation of the boundary-layer velocity profile with H is studied by plotting curves of u/U versus H for various constant values of y/θ. The data in these two reports are in good agreement for values of y/θ above one.

An analysis of the data of references 1 and 2 revealed that for each airfoil the quantity $S\eta$ varied less than 20 percent throughout the region of turbulent flow. This variation appeared to be somewhat dependent upon Reynolds number and hence these data were not in close agreement with the equation presented by Gruschwitz. However, for Reynolds numbers of several million the average variation for each configuration investigated was well represented by

$$\frac{\theta}{S}\frac{d(S\eta)}{dx} = 0.005 - 0.009\,\eta \qquad (7)$$

which is essentially the Gruschwitz equation. This equation was investigated only for regions of decreasing pressure coefficient S. It can be used to calculate the turbulent boundary-layer separation point for airfoils at moderate angles of attack. The value of η for which fully turbulent flow starts is approximately 0.58 (H = 1.4), and separation occurs when η attains a value of about 0.93 (H = 2.5). In performing this computation, it is merely necessary to know the chordwise pressure distribution. When the region of separated turbulent flow is more than 10 percent of the chord in length, there is a substantial difference between the actual and the potential-theory pressure distributions. Consequently, if the calculations are based on the potential-theory pressure distribution, considerable error can exist in estimating the chordwise position of the separation point. However, since, as was noted above, there is only a moderate chordwise variation in the quantity $S\eta$, it is possible to obtain a close estimate of the value of the pressure coefficient S over the separated region. In fact, a useful rough approximation is

$$(S\eta)_{\eta=0.58} \simeq \frac{6}{5}\,(S\eta)_{\eta=0.93}$$

or

$$\frac{S_{H=1.4}}{S_{H=2.5}} \simeq 2 \simeq \frac{U^2_{H=1.4}}{U^2_{H=2.5}}$$

which emphasizes that turbulent separation, just like laminar separation, is primarily a result of decreases in the pressure coefficient S.

The chordwise variation of η (or H) is of interest for evaluating changes in the velocity profile shape as well as for predicting separation. An interesting approximation for these velocity profiles can be obtained as follows:

Assume that the velocity distribution through the boundary layer is related by a power law to the distance from the surface, namely,

$$\frac{u}{U} = \left(\frac{y}{\delta}\right)^N$$

From the definitions of the various quantities it follows that

$$\frac{\theta}{\delta} = \frac{N}{(1+N)(1+2N)} \; ; \quad \frac{\delta^*}{\delta} = \frac{N}{N+1} \; ; \quad H = 1 + 2N$$

and hence

$$\frac{u}{U} = \left\{ \frac{y}{\theta}\left[\frac{N}{(1+N)(1+2N)}\right] \right\}^N \tag{8}$$

This simple expression is in surprisingly close agreement with the experimental data. The Gruschwitz shape parameter is then

$$\eta = 1 - \left(\frac{u}{U}\right)^2_{y=\theta} = 1 - \left[\frac{N}{(1+N)(1+2N)}\right]^{2N} \tag{9}$$

The variation of η with H given by this expression is shown in figure 3, which agrees satisfactorily with the curve obtained empirically by Gruschwitz. A further indication of the value of using η as a parameter is that the variation of skin-friction coefficient with η is linear for the data presented by Dryden. These data indicate a relation between the skin-friction coefficient and the boundary-layer shape factor such as

$$\frac{\tau_o}{2q} = \frac{\overline{\tau}_o}{2q}(2.8 - 3\eta)$$

where $\frac{\overline{\tau}_o}{2q}$ is the flat-plate skin-friction coefficient.

The turbulent separation on an NACA 66,2-216, a = 0.6 airfoil section at 10.1° angle of attack and a Reynolds number of 2.6 million

is analyzed in reference 2. The experimental pressure distribution for this airfoil is shown in figure 1. The growth of the momentum thickness in the turbulent region is computed by means of equation (5) and the experimental pressure distribution. The values obtained in this computation are substituted in equation (7) and the chordwise variation of η and hence H evaluated. These values of H and also the calculated values of momentum thickness are compared with the experimental data in figure 4. Although the computed values of H are smaller than those measured experimentally, the curves are similar in shape, and the fact that turbulent separation is imminent at the 0.7 chord station is predicted by the theory.

ANALOGIES BETWEEN BOUNDARY-LAYER FLOW AT TRANSONIC AND AT LOW SPEEDS

A number of the concepts which were developed in the preceding section for low-speed flows will be shown to apply in compressible flow. Recently Ackeret, Feldmann, and Rott (reference 4) published a thorough experimental investigation of boundary-layer flow in the vicinity of compression shock waves. These data will now be examined in the light of the preceding low-speed analysis. At transonic speeds the flow over an airfoil may be divided into three regions: the forward subsonic region, followed by a supersonic region terminated by a compression shock which returns the local flow to subsonic speeds. It is the character of the return of the flow from supersonic to subsonic velocity which varies with the state of flow in the boundary layer.

Laminar Flow

Consider first the case of laminar boundary-layer separation in the vicinity of a compression shock wave. When the boundary layer immediately ahead of the shock wave is laminar and the local Mach number is about 1.2 or greater, the compression shock wave is shaped like the Greek letter λ. The front leg of the λ is an oblique shock wave arising from the deflection of the boundary layer from the surface, that is, laminar separation. The rear leg is the main compression wave through which the flow goes from supersonic to subsonic velocity. Between these two branches of the shock wave the surface static pressure remains constant, a characteristic property of regions of laminar separation. Ackeret, Feldmann, and Rott present boundary-layer measurements for this type of flow. No measurements of the local velocity within the bubble of separation are presented. They assume appreciable negative velocity to exist in this bubble; whereas these velocities should be considered negligible. The boundary-layer-momentum and

displacement-thickness distributions were recalculated for zero velocity in the dead-air bubble. In performing these recalculations, the Ackeret procedure was used for obtaining the approximate density variation through the boundary layer from the measured Mach number distribution. This procedure is based on the assumption that energy is constant through the boundary layer. These revised experimental values are shown in figure 5. It is seen that over the constant-pressure region the displacement thickness grows approximately linearly (a phenomenon to be discussed later), while the momentum thickness remains virtually constant. Over the transition region of rapid pressure recovery, at the base of the main shock wave, displacement thickness remains constant but momentum thickness increases. The boundary-layer behavior in these regions is similar to that previously noted for low-speed laminar separation and transition. Moreover, at Mach numbers of about 1.2 the length of the constant-pressure region can be characterized by a Reynolds number run of 100,000, a value four times that observed at low speeds. This particular numerical value is characteristic of every case of transonic laminar separation presented in reference 4. The difference between the length of the laminar separated region at low and high speeds may be due to the increase in the stability of laminar flow with Mach number (reference 8).

Another analogy between transonic and low-speed laminar separation is the local flow deceleration which is associated with the onset of laminar separation. Von Karman and Millikan have shown that at low speeds laminar separation occurs at the point where $U^2_{separation}/U^2_{maximum}$ attains a certain numerical value. This value depends only upon the chordwise position of the maximum local velocity and, for cases in which this position is well removed from the leading edge, the numerical value of the ratio is approximately 0.88. This analysis could be expected to apply at transonic speeds because $U^2/2$ is the kinetic energy per unit mass of fluid in compressible as well as incompressible flow. The numerical value of this ratio for the transonic pressure distribution shown in figure 5 is 0.92 which is in satisfactory agreement with the low-speed analysis. Moreover, this ratio corresponds to a flow deflection of 1.5° when supersonic oblique-shock-wave theory is applied. In figure 5, this value is presented as the theoretical curve for the growth of the boundary-layer displacement thickness over the region of laminar separation. The theoretical variation of the displacement thickness is seen to be only about one-half of that found experimentally. This difference is primarily due to the curvature of the surface. The flow is deflected 1.5° with reference to a line tangent to the surface at the point of deflection. Consequently, in addition to the increase in displacement thickness caused by the flow deflection, there is an increase

measured by the perpendicular distance from the surface to the line tangent to the surface at the deflection point. It was not possible to determine this distance from the data presented in reference 4. A more exact calculation would consider this effect of surface curvature and then assume that δ^* is constant over the following transition region. The momentum thickness is theoretically constant over the region of laminar separation while the experimental measurements show a small increase. In the region of transition and reattachment, which occurs at the base of the main shock wave, the transonic data indicate that the displacement thickness is virtually constant. This result is the same as that noted for low-speed flow.

In order to calculate the growth of the boundary-layer momentum thickness in the transition region, it is necessary to employ the momentum integral equation. For a compressible fluid, this equation is

$$\frac{d\theta}{dx} + \frac{\theta}{\rho}\frac{d\rho}{dx} + \frac{2\theta+\delta^*}{2U^2}\frac{dU^2}{dx} = \frac{\tau_o}{2q} \tag{10}$$

where ρ and U are, respectively, the local density and velocity immediately outside the boundary layer. In the transition region, the flow is detached from the surface so the skin-friction coefficient is zero. As a first approximation to the density variation outside the boundary layer adiabatic variation is assumed. Then the solution of equation (10) is

$$\left(\frac{\delta_1^*+K\theta_1}{\delta_1^*+K\theta_2}\right)^{1/K} = \frac{M_2^*}{M_1^*}$$

where subscripts 1 and 2 are, respectively, conditions at the beginning and end of an interval in which K is the average value of

$$K = \frac{12-7M^{*2}}{6-M^{*2}}$$

The momentum-thickness distribution calculated, by means of this approximate solution, over the transition region is also presented in figure 5.

A further effect of laminar separation, which is indicated by Ackeret's data, is a rearward movement of the position of the main shock wave from its position when the boundary layer is turbulent. Consider the subsonic chordwise velocity distribution behind the shock wave in the latter case as a reference distribution; it is apparent that the presence of the effective bump, which is the bubble

of laminar separation, raises the local velocities above the reference distribution. Thus, the chordwise location of the point at which sonic velocity occurs moves aft, and hence the shock wave moves aft when fully turbulent boundary-layer flow is replaced by laminar separation. It should be noted that between these two types of shock-wave boundary-layer interaction there is another possible type. When laminar separation occurs some distance from the leading edge of an airfoil, the laminar boundary layer at the separation point is rather thick and easily destabilized. Thus, the very process of laminar separation could precipitate transition ahead of the main shock wave. This would result in a marked change in the appearance of the main shock wave from that of the lambda-type wave.

The question arises as to whether the boundary-layer momentum integral equation can be used to calculate the boundary-layer growth through a shock wave. The primary factor which could invalidate the use of this equation would be the occurrence of static pressure variation through the boundary layer. In reference 4, static pressure surveys through the boundary layer are presented. The experimental measurements show that the static pressure is virtually constant through the boundary layer even when there is a large static pressure gradient immediately outside the boundary layer. Equation (10) is therefore applicable. However, before attempting a solution of this equation for turbulent flows, it is necessary to investigate the characteristics of turbulent boundary layers at high speeds.

Turbulent Flow

The transonic, turbulent-boundary-layer velocity profiles presented by Ackeret can be analyzed by the methods used for low-speed turbulent velocity profiles. The variable considered was the ratio of the local velocity at various points inside the boundary layer to the local velocity immediately outside the boundary layer. The points for which the local velocity ratio was considered were at a distance y from the airfoil surface equal to the local momentum thickness θ, and also at even integral multiples of this distance y/θ from the surface. The latter points are plotted against the former in figure 6. The curves drawn in this figure were obtained for low-speed turbulent boundary layers. The data for a value of y/θ of 4 indicate that the boundary-layer velocity profiles at transonic speeds may differ somewhat from those at low speed over the outer portion of the profiles. However, at the inner portion of the boundary layer, the values for transonic speeds are in agreement with the curves obtained from low-speed data. It therefore follows that essentially the same boundary-layer velocity profiles occur at low and transonic speeds, and throughout this Mach number range the same Gruschwitz shape parameter η applies.

The relation between η and δ^*/θ (or H) is different for compressible and incompressible flows because of the variation of density through the boundary layer. Ackeret assumes that the total energy and static pressure are constant through the boundary layer. From this it follows that the density variation through the boundary layer is a function of the velocity-profile shape, the free-stream Mach number, and the local stream Mach number M. Values of H have been calculated for free-stream Mach numbers between 0.7 and 1.0, and various local Mach numbers. As long as the local Mach number is greater than the free-stream Mach number but less than 1.4, the effect of compressibility on the value of H is well approximated by

$$H = H_{M=0}\left(1 + \frac{2}{5}M^2\right) \tag{11}$$

It is now possible to consider solutions of equation (10) which can be used to calculate the turbulent-boundary-layer growth through a shock wave. The pressure and Mach number variation in this region are large, and both of these factors have appreciable effects on H. The pressure variation causes an increase in H, the magnitude of which is reduced as a result of the decreasing local Mach numbers. This suggests the simple approximation of again using a constant average value of H in solving the momentum integral equation. This is such a gross approximation that it would be foolish to attempt to include the relatively small effect of the surface shear forces. Assuming a constant average value of δ^*/θ and neglecting the surface shear forces, equation (10) reduces to

$$\theta\rho U^{(2+H)} = \text{constant} \tag{12}$$

This same equation has been employed (reference 9) for estimating the increase in boundary-layer momentum thickness through the trailing-edge shock wave of an airfoil at supersonic speeds.

It is necessary to calculate the chordwise variation of both H and the momentum thickness θ before an estimation of the growth of the displacement thickness δ^* may be made. As has been previously discussed, an analysis of the turbulent transonic boundary layers of reference 4 (fig. 6) indicated the applicability of the parameter η for specifying the shape of the boundary layer. Therefore, the data of reference 4 were analyzed in terms of equation (7) of this report. In performing this analysis, equation (7) was written in the form

$$\frac{\theta}{U^2}\frac{d(\eta U^2)}{dx} = 0.005 - 0.009\,\eta \qquad (13)$$

and used with the experimental values of θ and M* to calculate the variation of η. The calculated and experimental values of η are compared in figure 7. With the chordwise variation of η known, values of $H_{M=0}$ may be determined from equation (9) or figure 3. Equation (11) gives the correction to $H_{M=0}$ for the effect of compressibility. Since H equals δ^*/θ, δ^* is immediately available.

To illustrate these results, a typical example, taken from reference 4, is presented in figure 8. The calculations were based on the experimental static pressure distribution which was converted to velocity distribution by using Bernoulli's equation for adiabatic flow. At the peak pressure, the value of H was obtained from equation (11) under the assumption that $H_{M=0}$ would have been 1.4. This value of H was used in equation (12) to calculate the momentum-thickness distribution shown in figure 8. Equation (13) then gave the chordwise variation of η. Figure 3 was used to convert the calculated values of η to $H_{M=0}$ and equation (11) to determine the corresponding values of H. Since H equals δ^*/θ, δ^* was easily determined. These values are also compared with the experimental measurements in figure 8.

The data presented by Ackeret indicate an important fact regarding the variation of the turbulent-boundary-layer profile shape through the shock wave. In the immediate vicinity of the shock wave, the large pressure gradient causes the velocity profile to approach the shape associated with turbulent separation in low-speed flows. However, immediately following this region is one with much smaller pressure gradients, and in this latter region the boundary-layer velocity profile tends to return to a shape characteristic of unseparated turbulent boundary layers. This tendency to return to a flat-plate type of velocity profile is indicated, by equation (13) and figure 7, to be characteristic of regions of small pressure gradients. It thus appears possible that immediately behind a sufficiently intense shock wave the boundary layer may be separated, but re-establishment of turbulent boundary-layer flow will occur if the subsonic region behind the shock is sufficiently extensive and if the adverse pressure gradient over that region is small.

DISCUSSION AND CONCLUDING REMARKS

In the preceding analysis, a general similarity has been found between boundary-layer flows at low speeds and transonic speeds. The low-speed case considered was an airfoil section at moderate

angle of attack; the transonic case was a surface over which there was a rather extensive region of supersonic flow. The comparison of the various flow regimes for these two cases will now be discussed.

Laminar separation in the low-speed case is due to the adverse pressure gradient aft of the sharp leading-edge pressure peak. The potential-theory pressure distribution is so modified by the presence of separation that locally the pressure gradient is zero. The extent of the zero-gradient region is such as to permit the laminar flow to turn turbulent and is characterized by a Reynolds number run of approximately 25,000. At transonic speeds laminar separation is more complex because the occurrence of an adverse gradient and laminar separation are two aspects of the same physical phenomena; that is, it is not apparent that one is cause and the other effect. However, the magnitude of the flow deceleration immediately ahead of separation is the same as for low-speed flows, and in the latter case it is known that this flow deceleration causes laminar separation.

The examples of transonic flow considered in the present report have a more extensive length of laminar flow ahead of the transition point and hence a thicker boundary layer than the low-speed examples. Consequently, the transonic disturbance which causes laminar separation at one Reynolds number can cause abrupt transition at a somewhat larger Reynolds number. For moderate Reynolds numbers (about one million) and Mach numbers of about 1.2 the length of the laminar-separation region is characterized by a Reynolds number run of about 100,000.

At both low and transonic speeds, the boundary-layer momentum thickness remains constant over the constant-pressure region, and the displacement thickness grows in such a manner as to effectively change the local surface shape to one over which the pressure gradient would be zero. When transition occurs, there is a large pressure gradient and considerable pressure recovery before the separated flow reattaches to the surface as a turbulent boundary layer. It does not seem to have been recognized previously that such a large pressure recovery occurs over the transition region before the onset of fully developed turbulent boundary-layer flow. In the transition region the boundary-layer displacement thickness is relatively constant, while the momentum thickness increases markedly.

The velocity distributions through turbulent boundary layers at low and transonic speeds appear to belong to the same one-parameter family. Thus, specifying the ratio of the local stream velocity to the velocity at a distance from the surface equal to

the local momentum thickness immediately specifies the entire velocity profile. This property of turbulent boundary layers suggests the use of the Gruschwitz method for calculating the chordwise variation of the velocity-profile shape. The available data indicate that such calculations give results in fair agreement with experimental measurements at both low and transonic speeds.

A rough approximation determined from the Gruschwitz equation for the magnitude of the flow deceleration which is sufficient to cause an initially fully developed turbulent boundary layer to separate is

$$\left(\frac{U_{separation}}{U_{initial}}\right)^2 = \frac{1}{2}$$

It thus follows that if the boundary layer is turbulent ahead of a shock wave, and through the shock the local Mach number goes subsonic from a moderate supersonic value, then separation may exist behind the shock. However, the turbulent boundary layer re-establishes itself as unseparated flow if the adverse pressure gradient behind the shock is sufficiently small. This important effect of the pressure gradient existing behind the shock wave suggests that airfoil sections having small pressure gradients over the rear portion of the chord will have better flow characteristics at transonic speeds than airfoils having large gradients in this region.

The question arises as to whether the magnitude of the peak local Mach number occurring on airfoils is limited by flow separation. The available data give no answer to this problem. However, the analysis indicates that, if turbulent boundary-layer flow exists ahead of the shock, the maximum deceleration through the shock compatible with the stability of the turbulent boundary layer corresponds to a decrease in Mach number from 1.5 to 1.0. Thus, if the flow behind the shock is to be subsonic, the properties of the turbulent boundary layer appear to impose a limiting value of 1.5 for the peak Mach number.

The rather rudimentary analysis of the present report cannot be considered as the answer to the various problems dealt with. It is rather intended to present a simple and coherent picture of the boundary-layer variation for certain airfoil configurations. The basic similarities between the low-speed and transonic-speed cases considered indicate that important simplifications and extensions of current boundary-layer theory are possible.

Ames Aeronautical Laboratory,
National Advisory Committee for Aeronautics,
Moffett Field, Calif.

REFERENCES

1. Dryden, Hugh L.: Some Recent Contributions to the Study of Transition and Turbulent Boundary Layers. NACA TN No. 1168, 1947.

2. von Doenhoff, Albert E., and Tetervin, Neal: Determination of General Relations for the Behavior of Turbulent Boundary Layers. NACA ACR No. 3G13, 1943. TR 772

3. Gruschwitz, E.: Die Turbulente Reibungsschicht in Ebener Stromung Bei Druckabfall und Druckansteig. Ing-Archiv, vol. 2, no. 3, Sept. 1931, pp. 321–346.

4. Ackeret, J., Feldmann, F., and Rott, N.: Investigations of Compression Shocks and Boundary Layers in Gases Moving at High Speed. NACA TM No. 1113, 1947.

5. von Kármán, Th., and Millikan, C. B.: On the Theory of Laminar Boundary Layers Involving Separation. NACA TR No. 504, 1934.

6. von Doenhoff, Albert E., and Tetervin, Neal: Investigation of the Variation of Lift Coefficient with Reynolds Number at a Moderate Angle of Attack on a Low-Drag Airfoil. NACA CB, Nov. 1942.

7. Falkner, V. M.: A New Law for Calculating Drag. The Resistance of a Smooth Flat Plate with Turbulent Boundary Layer. Aircraft Engineering, vol. XV, no. 169, Mar. 1943, pp. 64–69.

8. Allen, H. Julian, and Nitzberg, Gerald E.: The Effect of Compressibility on the Growth of the Laminar Boundary Layer on Low-Drag Wings and Bodies. NACA TN No. 1255, 1947.

9. Ivey, H. Reese, and Klunker, E. Bernard: Considerations of the Total Drag of Supersonic Airfoil Sections. NACA TN No. 1371, 1947.

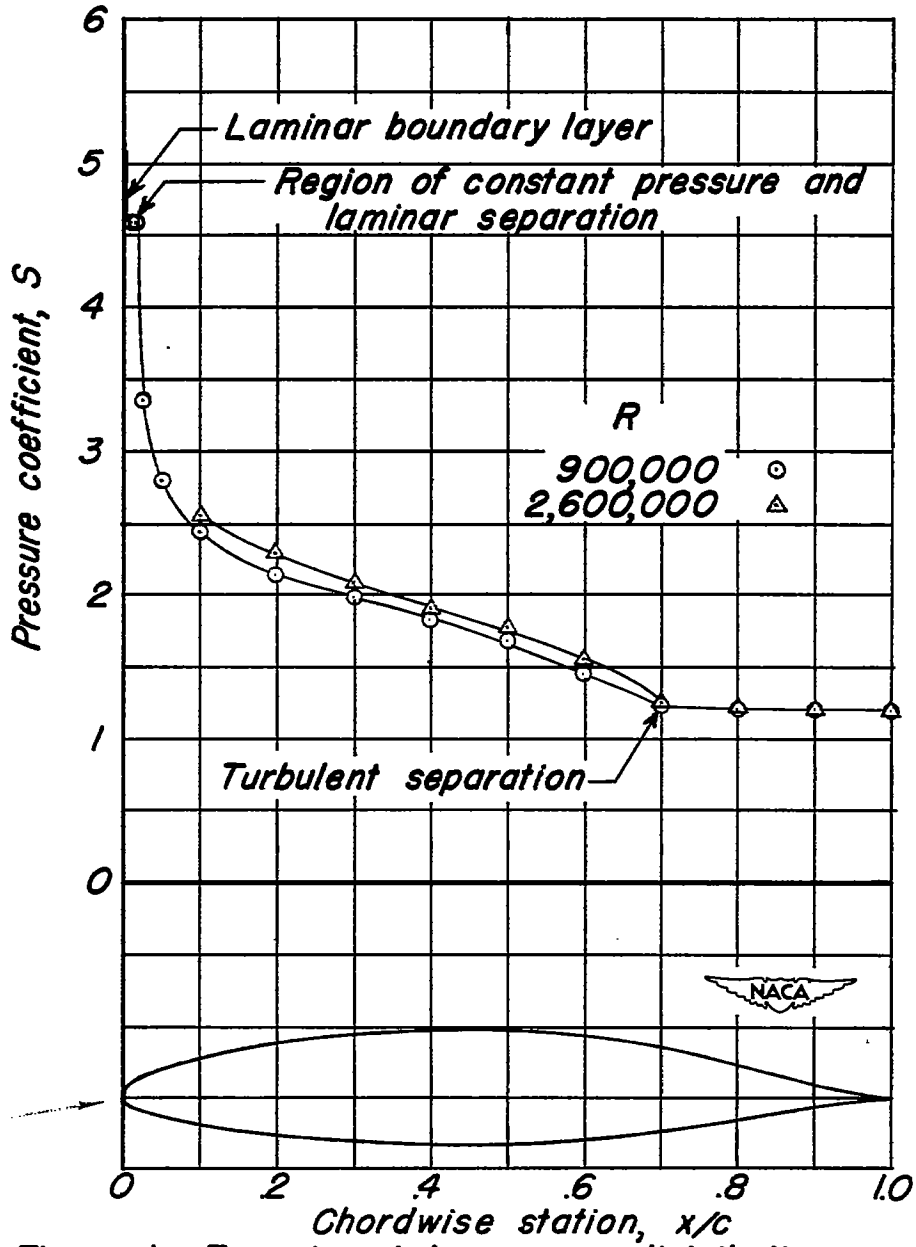

Figure 1.- Experimental pressure distribution over upper surface of an NACA 66,2-216, a=0.6 airfoil section. α, 10.1°. (Data from reference 6)

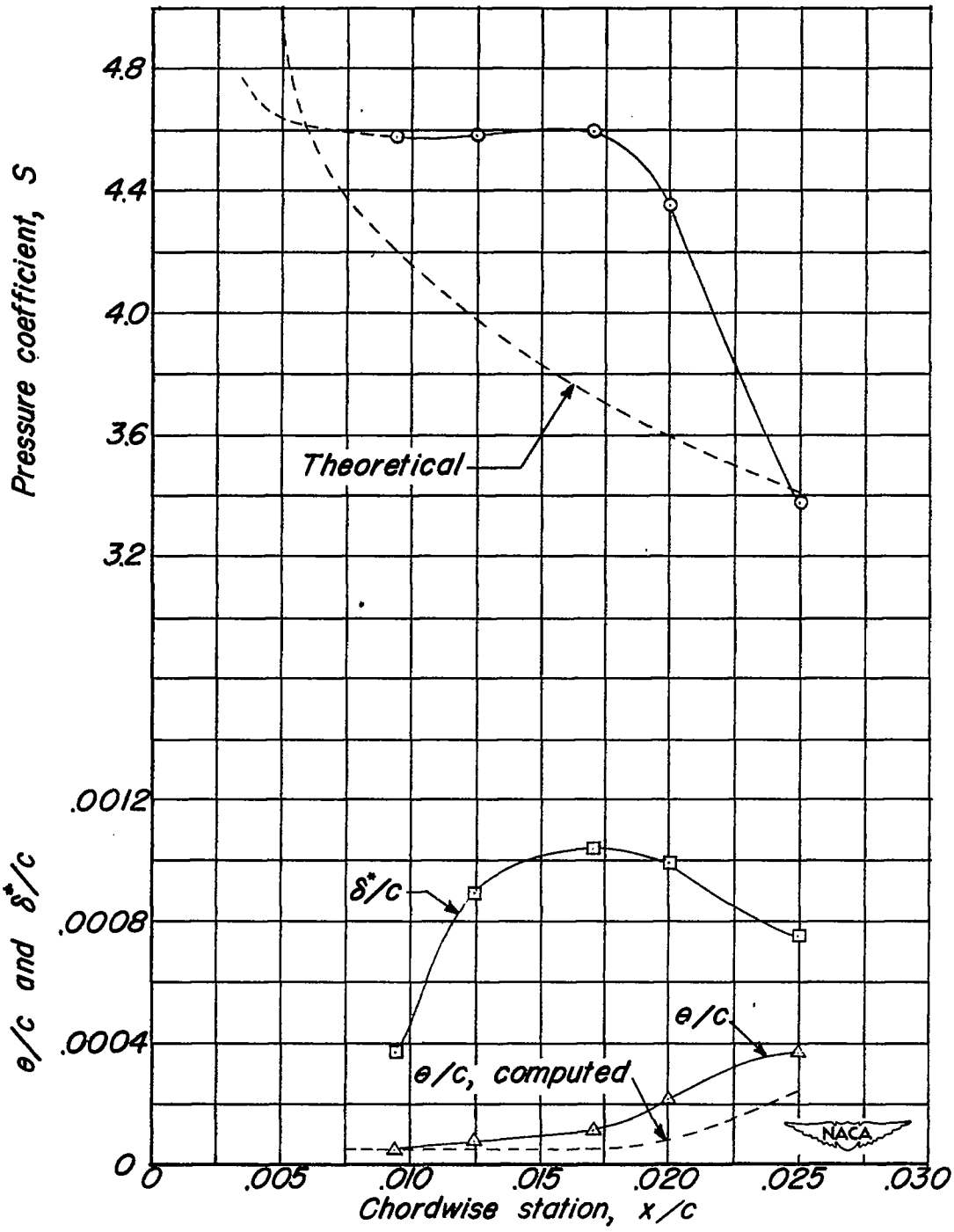

Figure 2.- Variation of pressure coefficient and boundary-layer momentum and displacement thicknesses over upper surface of airfoil leading edge. Airfoil section, NACA 66,2-216, a=0.6; R, 900,000; α, 10.1°. (Data from reference 6)

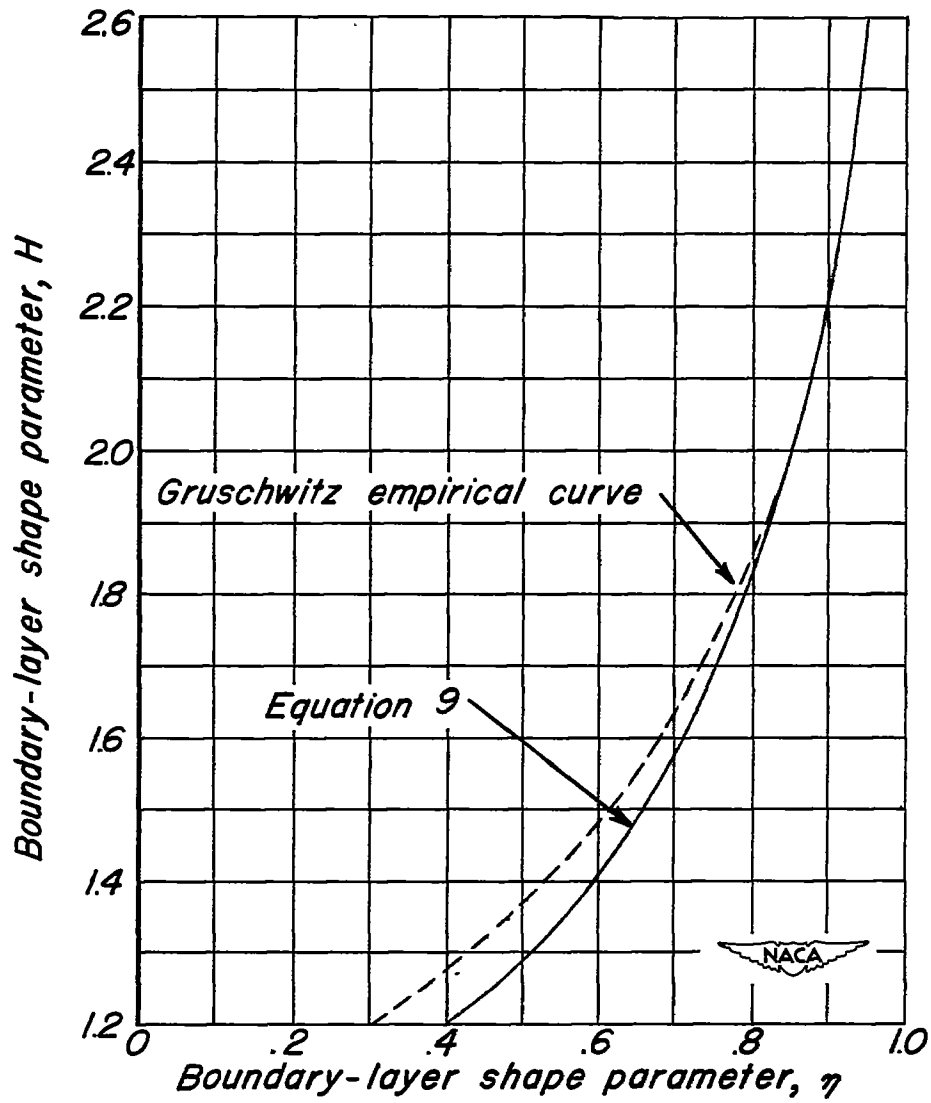

Figure 3.—Variation of H with η.

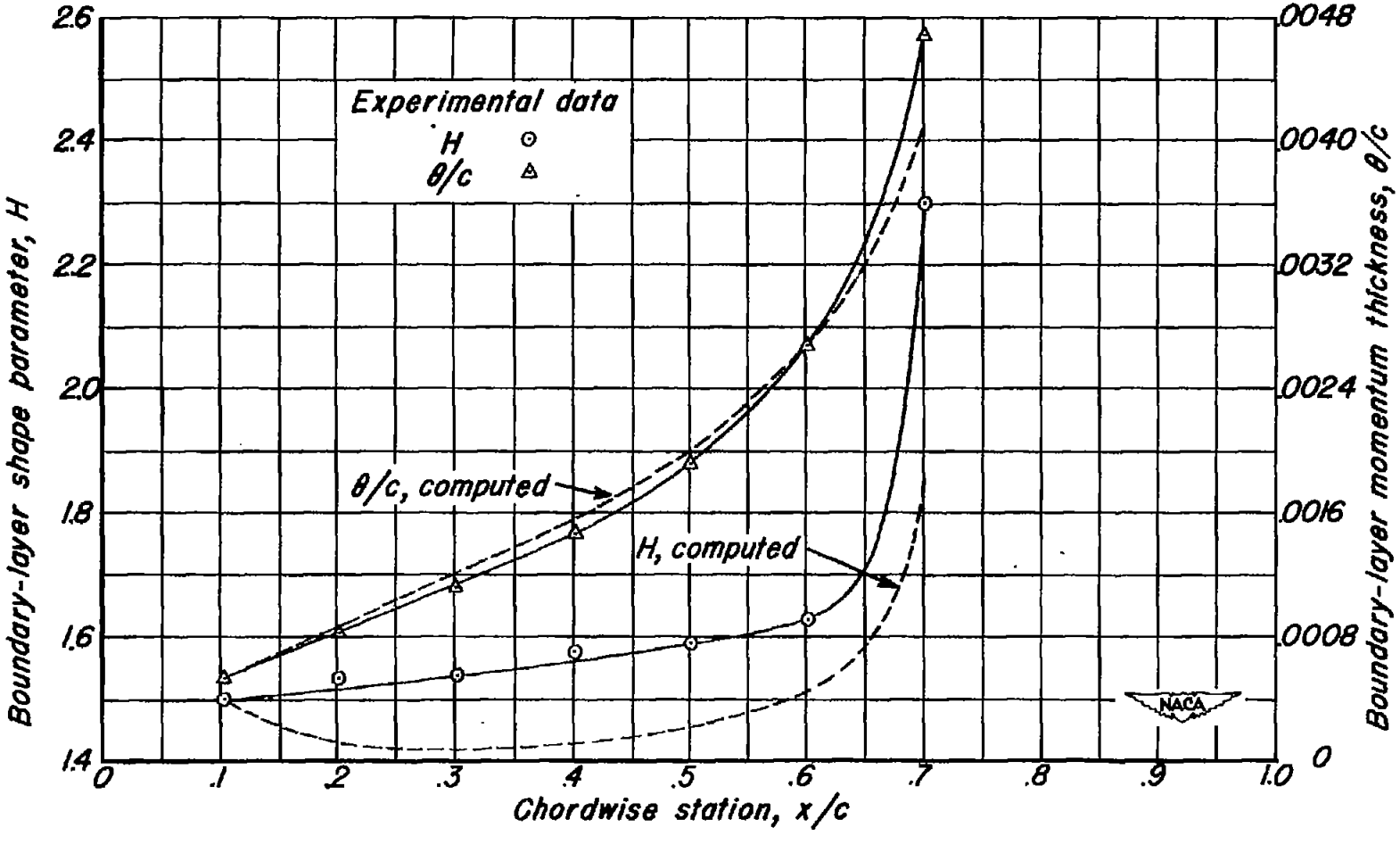

Figure 4.– Experimental and calculated values of H and θ/c for a NACA 66, 2–216, a=0.6 airfoil. R, 2,600,000; α, 10.1°. (Data from reference 2)

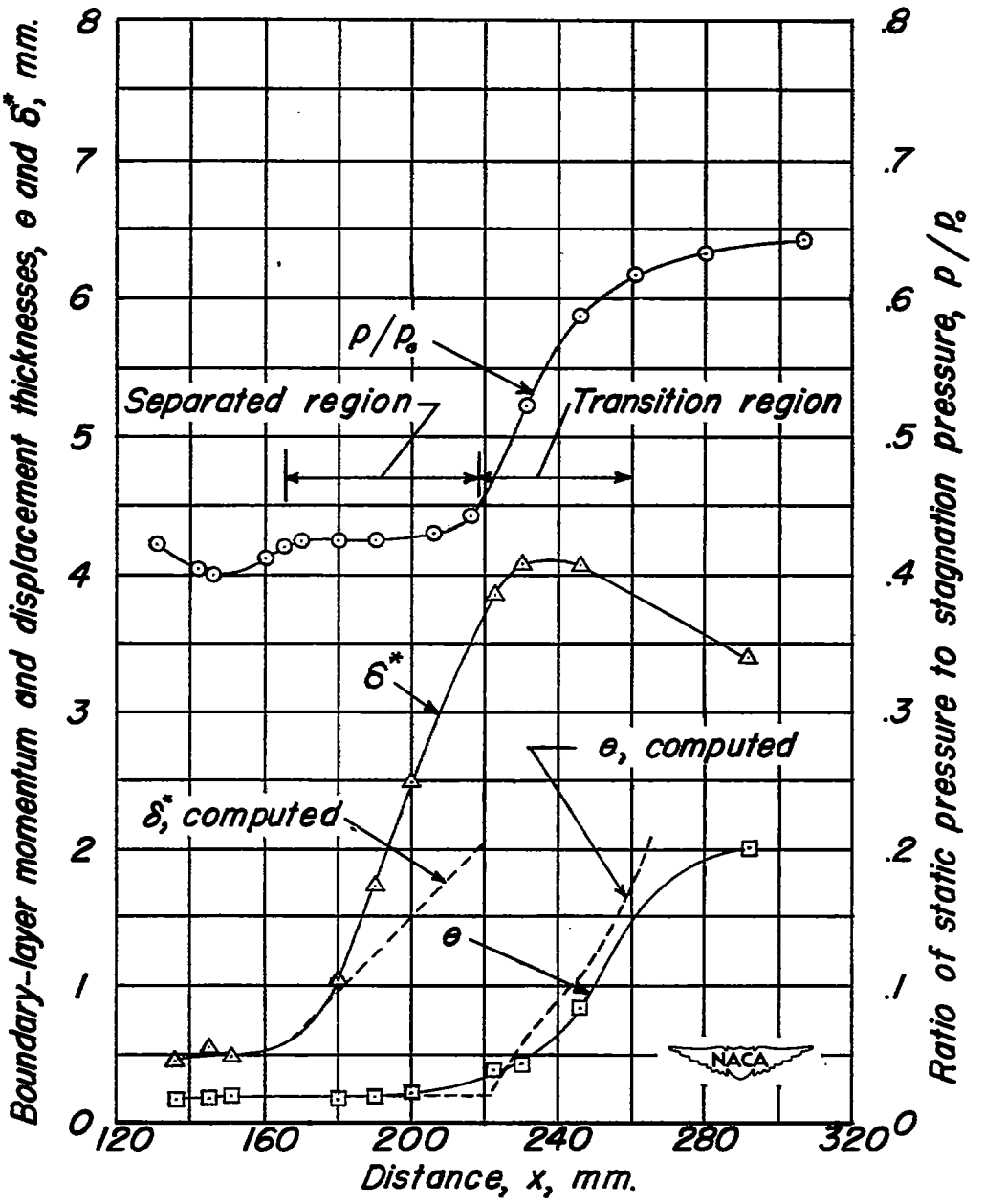

Figure 5.– Distribution of boundary-layer momentum and displacement thicknesses and the ratio of static pressure to stagnation pressure through a lambda type shock wave. Mach number before shock wave, 1.225. (Data from reference 4)

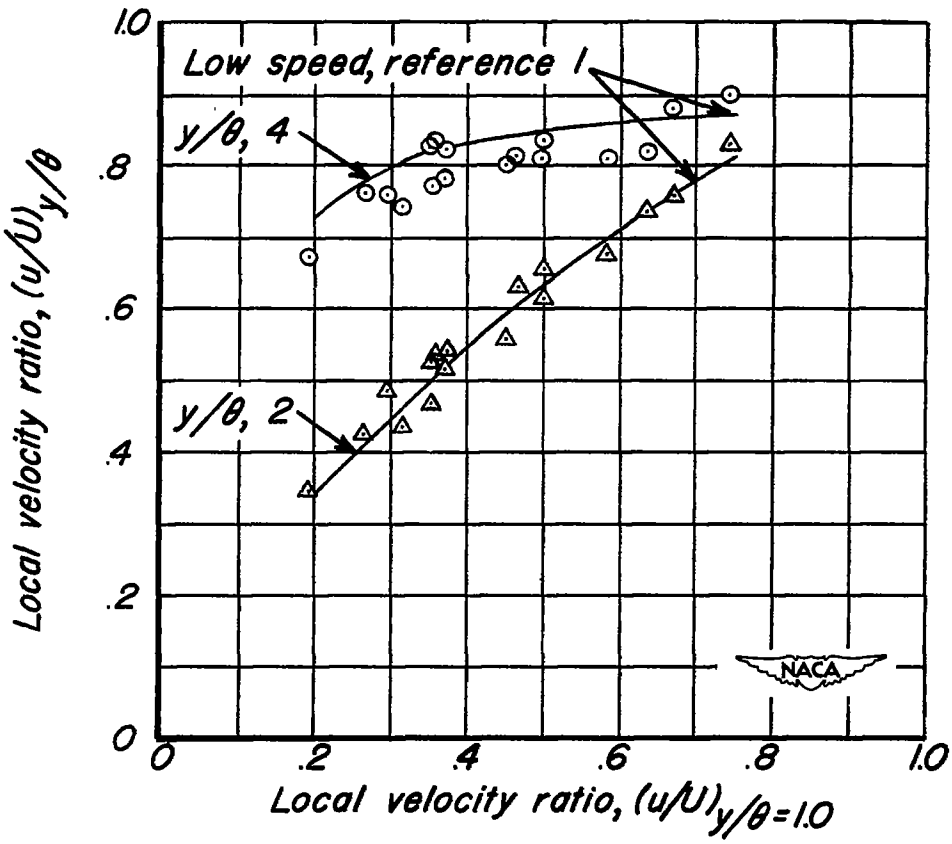

Figure 6.– Comparison of low speed and transonic boundary-layer profiles.

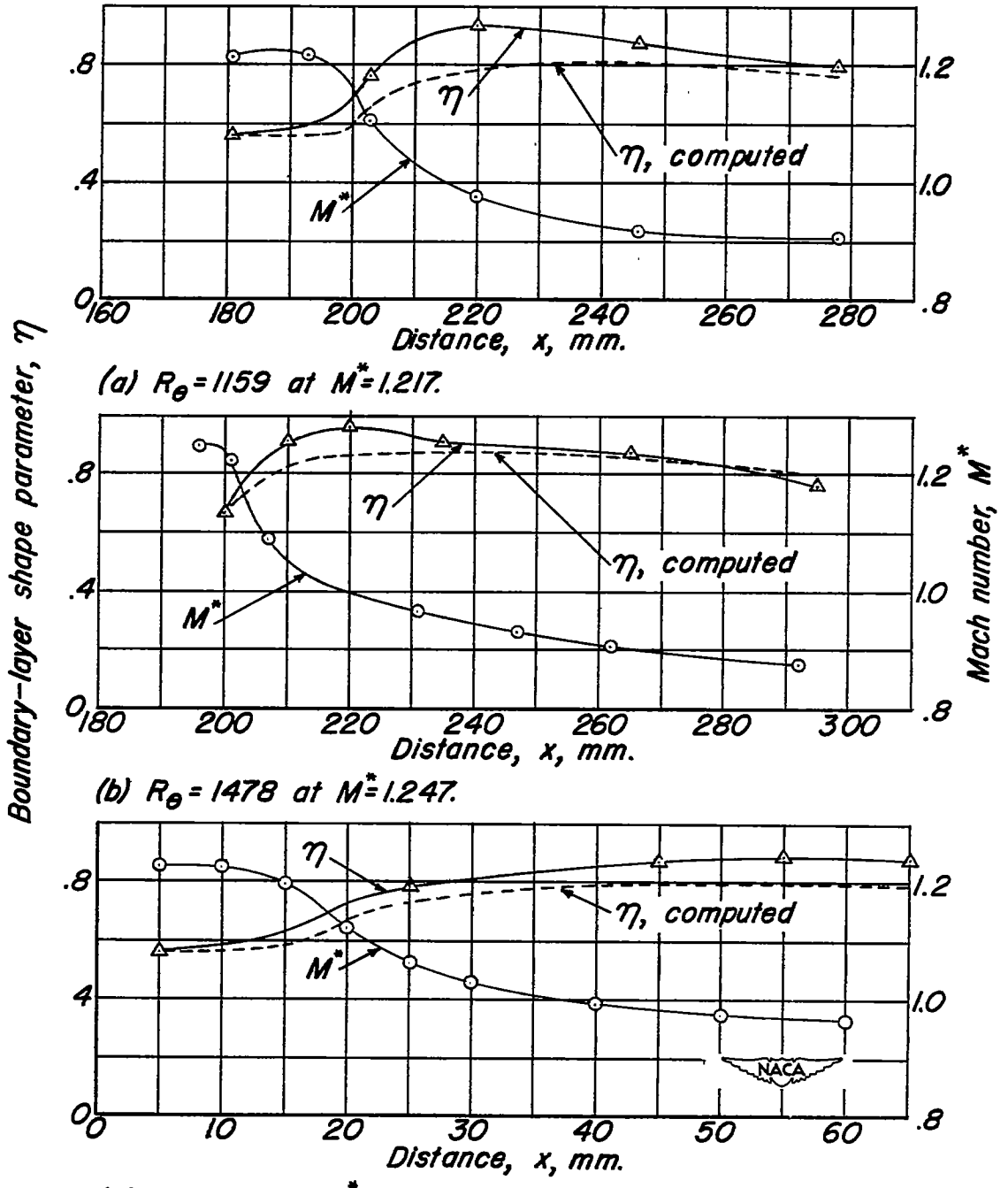

Figure 7.—Variation of boundary-layer shape parameter, η, through compression shock waves. Turbulent boundary layer ahead of shock. (Data from reference 4)

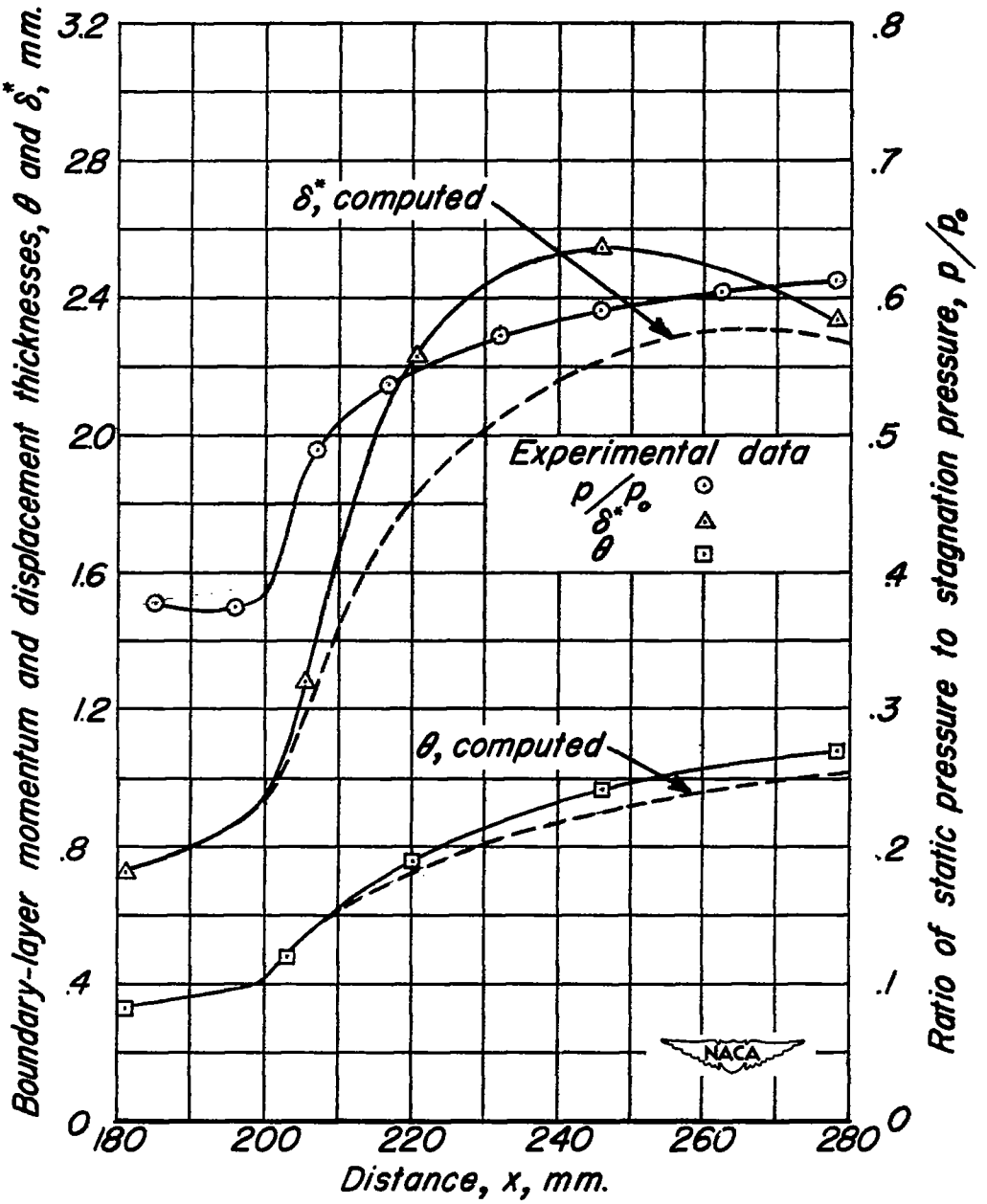

Figure 8.– Distribution of boundary-layer momentum and displacement thicknesses and the ratio of static pressure to stagnation pressure through a shock wave for the case of a turbulent boundary layer. Mach number before shock, 1.279. (Data from reference 4)